PROPOSAL SUMMARY

MEASUREMENTS OF HIGH ENERGY COSMIC RAY SPECTRA ABOVE 100 GeV

PRINCIPAL INVESTIGATOR/INSTITUTION: James H. Adams, Jr./NRL

CO-INVESTIGATORS/INSTITUTIONS:

Dr. A.V. Apanasenko/Lebedev Inst.
Prof. N.L. Grigorov/Moscow State U.
Prof. M.I. Panasyuk/Moscow State U.
Dr. V.I. Zatsepin/Moscow State U.

The objective of this investigation is to determine if the galactic cosmic ray spectra deviate form a power law in energy between 100 GeV and 10 TeV. At an energy of about 1 TeV/n the galactic cosmic ray spectra measured by different techniques join, but do not necessarily coincide. The spectra below 1 TeV/n have been measured by various electronic detector techniques and above a few TeV/n the spectra have been measured mostly by passive calorimeters. We propose two tests to determine if the spectra follow a simple power law in this region or if there is a change in the spectral slope as some measurements suggest. The first test is to make an accurate measurement of the all particle spectrum from 100 GeV to 10 TeV to see if this composite spectrum follows a simple power law. The second test is to investigate in detail the operation of two designs of passive calorimeters in the region of their detection threshold. We intend to determine how the difference in the designs affects their cosmic ray detection efficiency just above their detection thresholds.

This is a new proposed investigation which has not been supported by NASA's SRT program previously.

We propose to fly two experiments on a long duration balloon flight around the north pole that is being planned for the summer of 1995. The first of these experiments will be an active thin cosmic ray calorimeter which will be used to measure the cosmic ray all particle spectrum. The second will consist of passive thin calorimeters in the configurations used by the Japanese American Cooperative Emulsion Experiment (JACEE) collaboration and by the Moscow University Balloon Emulsion Experiment (MUBEE) collaboration. All these instruments exist and have been flown on test flights in Northern Canada. We plan to design and build a gondola for these instruments and also an interface between the active instrument and the data system provided by NASA so that the data can be returned by satellite during the flight. We expect to support payload integration, flight operations and recovery operations.

The investigation of the high energy cosmic ray spectra from 10^{11} to 10^{16} eV is the highest priority research goal in NASA's cosmic ray program. The aim of this is to search for features in the cosmic ray energy spectra that may reveal the nature of the mechanism responsible for the acceleration of galactic cosmic rays. The focus of the investigation proposed here is to be sure that no spectral feature has been overlooked in the energy range from 10^{11} to 10^{13} eV which contains the juncture where the measuring technique changes.

1.0 PROJECT DESCRIPTION

ABSTRACT

At an energy of about 1 TeV/n the galactic cosmic ray spectra measured by different techniques join. The spectra below 1 TeV/n have been measured by various electronic detector techniques and above a few TeV/n the spectra have been measured by passive calorimeters. We propose two tests to determine if the spectra follow a simple power law in this region or if there is a change in slope. The first test is to make an accurate measurement of the all particle spectrum from 100 GeV to 10 TeV to see if this composite spectrum follows a simple power law. The second test is to investigate in detail the operation of two designs of passive calorimeters in their threshold region to determine how the designs affect the cosmic ray detection efficiency just above their detection thresholds.

We propose to fly two experiments on a long duration balloon flight around the north pole in the summer of 1995. The first of these experiments will be an active thin cosmic ray calorimeter which will be used to measure the cosmic ray all particle spectrum. The second will consist of passive thin calorimeters in the configurations used by the Japanese American Emulsion Experiment collaboration and by the Moscow State University group. All these instruments exist and have been flown on test flights in Northern Canada. We plan to design and build a gondola for these instruments and also an interface between the active instrument and the data system provided by NASA so that the data can be returned by satellite during the flight. We expect to support payload integration, flight operations and recovery operations.

1.1 Introduction

The most striking feature of the galactic cosmic ray all particle spectrum is that it extends over twelve orders of magnitude in energy without a single discontinuity. Air shower measurements indicate that the all particle spectrum contains one strong feature, the "knee" which occurs just below 10^{16} eV. Could it be that there is a single mechanism responsible for accelerating particles over such a vast span of energy? Theoretical models of particle acceleration in astrophysical settings suggest that two or more mechanisms are required and predict the existence of spectral features at energies where there is a transition from one dominate mechanism to another. There are also models which suggest effects in the cosmic ray sources that would cause additional features in the spectrum. The mechanism for cosmic ray confinement by the magnetic fields of the galaxy will also contribute features to the individual cosmic ray elemental spectra. The "knee" probably marks the energy of some major change in the cosmic ray source or confinement mechanisms, but it is probably not the only significant feature in the cosmic ray spectra. It is quite possible that significant features exist in the cosmic ray elemental spectra at energies that are currently accessible to direct observation. The search for such features has been given a high priority in NASA's cosmic ray program and it is the objective of this proposal.

1.2 Theoretical Predictions

Theoretical work on cosmic ray acceleration points to diffusive shock acceleration by supernova blast waves as the dominant mechanism at the energies that are currently accessible to direct measurements in space or on balloons (Drury et al., 1989). The most straight forward model for supernova blast wave acceleration suggests that this mechanism will loose its effectiveness at 10^{14} eV (Gaisser, 1990).

Upon closer examination, however, one must realize that the resulting spectral feature may not be sharp or even a single feature. The cosmic rays we observe at Earth are likely to be a mixture of particles accelerated by many supernova blast waves. The maximum energy achieved by each of these blast waves depends on its strength and duration as an effective accelerator. The strength and duration of different blast waves is likely do differ greatly both because of the size and character of the supernova and because of the inhomogeneity of the interstellar medium into which the blast wave expands. It should also be noted that supernova often occur in association and their blast waves intersect, creating "superbubbles" which may be capable of accelerating particles to higher energies.

The usual approach to modeling acceleration by supernova blast waves is to assume that the acceleration mechanism is diffusive acceleration across a quasi-parallel shock. Jokipii (1987) has pointed out that this may not be the most efficient mechanism. He shows that the combination of diffusion and drift acceleration in a quasi-perpendicular shock configuration can accelerate particles faster and more efficiently, achieving a limiting energy that is perhaps ten times higher for the same supernova.

With the range of possibilities discussed above, one can imagine that the spectral feature that marks the end of supernova blast wave acceleration could be a gradual one, spread over more than an order of magnitude in energy or it could contain subtle sub-features due to the occurrence of supernova blast wave acceleration in several distinct, but common circumstances.

There is also reason to believe that the breakdown of the supernova blast wave mechanism for acceleration may not be the only thing that can cause a feature in the part of the cosmic ray spectrum that is accessible to direct measurement. It is well established that between 4 and 100 GeV/n that it becomes increasingly easy for cosmic rays to escape their magnetic confinement region (presumably the disk of the galaxy). Gupta and Webber (1989) have shown that the escape mean free path from this confinement decreases with increasing magnetic rigidity as $R^{-0.6}$ for $R \geq 4$ GV. If we assume that this rigidity dependence continues to higher energies and extrapolate the escape mean free path to $3X10^{15}$ eV, the result implies that the residence time for cosmic rays in the galaxy is about 1000 years, i.e. on the order of the time to cross the disk! However cosmic rays at this energy, must not escape so freely from the confinement region because if they did the cosmic ray anisotropy at this energy would be much greater than the measured value of 0.1% (Gaisser, 1990). This certainly suggests that the escape mean free path cannot continue to decrease as $R^{-0.6}$, but must flatten off at some energy. When this happens, we should expect to see the effect as a feature, at least in the spectra of the secondary cosmic ray nuclei.

When we measure the cosmic ray spectra searching for features, we must be aware of such possibilities as have been suggested above. Even in the energy range from 10^{11} to 10^{14} eV which is currently being investigated, we may well find more than one feature.

1.3 Direct Measurements of The Cosmic Ray Spectra:

The direct measurements of the high energy cosmic ray spectra have been recently reviewed by Swordy (1993). There is general agreement that all the spectra are consistent with the simple leaky box model up to 1 TeV/n (Swordy et al., 1993; Buckley et al., 1994; Swordy et al., 1990;, and Muller et al., 1991). The only apparent exception to this is the spectrum of Si which falls off with increasing energy more steeply than the rest (Ichimura et al., 1993). Above 1 TeV, the elemental abundances above He are only reported as groups of elements. Swordy (1993) compares the measurements of the CNO, Ne-S and Fe group spectra reported by various authors. These data appear to indicate that all these spectra become flatter above 1 TeV/n. This just happens to be where the techniques used for measuring the spectra change. Below 1 TeV/n measurements are make with electronic detectors such as with thick active calorimeters (e.g., Ryan et al., 1972), transition radiation detectors (Muller et al.,1991) and ring imaging Cherenkov detectors (Buckley et al., 1994). Above this energy, the measurements are make predominately with thin passive calorimeters (e.g., Burnett et al, 1986; and Parnell et al., 1989). In his review, Swordy (1993) does include the data from the Sokol Experiment (Ivanenko et al., 1993) which is a active thick calorimeter. This version of the Sokol results is consistent with the rising spectral index measured with the passive calorimeters (Asakimroi et al., 1993), but the Sokol results are controversial. In a separate accounting of the results of Sokol, Grigorov (1990) reports measurements of the $Z > 5$ spectrum that are consistently lower. On the other hand, recent results from another passive calorimeter experiment (Zatsepin, 1993) are consistent with those of the JACEE experiment (Asakimori et al., 1993).

The helium spectrum (Buckley et al., 1994; and Swordy, 1993) also shows a discontinuity or perhaps a flattening near 1 TeV/n, again just at the point were the measuring techniques change. Zatsepin (1993) has compared in his figure 2 (which we reproduce here as figure 1), measurements above 1 TeV/nucleus from the JACEE passive calorimeters[8], Proton satellite[2] (Grigorov et al., 1970), the SOKOL experiment in two versions, (Ivanenko et al., 1990)[7] and (Grigorov, 1990)[6], the thick active calorimeter experiment[5] of Ryan et al. (1972) and his own passive calorimeters[1]. The data show a vertical spread that is statistically significant in some cases. In particular, it shows that the flattening in the helium spectrum above 1 TeV which is apparent in Swordy's review may be an instrumental effect associated with the change in detector technology at 1 TeV. Comparing Figure 12 of Buckley et al. (1994) with this figure it is apparent that the data from the RICH detector are more consistent with the results from Proton, Sokol (Grigorov, 1990) and the Russian passive calorimeter data. The fact that the active experiments tend to agree and that the passive experiment results appear to be significantly different, at least just above 10 TeV seems to suggest that there may be systematic effects in the passive technique that are not well understood.

Now we turn to the data on the proton spectrum. The current state of measurements of the proton spectrum was presented by Swordy (1993) in his review. The measurements above 1 TeV come mostly from two passive thin calorimeter groups (Zatsepin et al, 1993) and (Asakimori et al., 1993). Both data sets indicate a steepening of the proton spectrum above 1 TeV, but disagree on the location of the steepening. Zatsepin et al. claim that the spectrum steepens in the vicinity of 10 TeV while Asakimori et al. claim the spectrum remains flat up to 40 TeV and then steepens. Zatsepin have suggested that the higher energy for the steepening of the spectrum reported by Asakimori et al. could be due to the low flux at their first two data points which are near their detection threshold. In addition to the data from the two passive experiments, there is the data from the Sokol experiment which is reported in two versions. Both are shown in Zatsepin (1993) in his figure 1 (which is reproduced here as figure 2). Unfortunately, the Sokol data lacks the statistical precision and the consistency to resolve the discrepancy between the two passive experiments.

The only other data on the proton spectrum above 1 TeV are from the Proton 2, 3, and 4 satellite experiments (Akimov et al., 1969; Grigorov et al., 1972). The results of these experiments are represented by the solid line in figure 2 and fall off more steeply than the other measurements above 10 TeV. Ellsworth et al., 1977 have suggested that this difference is due to the effects of electrons backscattered from the calorimeter into the proportional counters that were used for charge measurement. Grigorov (1990) has examined this possibility by comparing Proton measurements with those from the Sokol instrument which was designed to strongly suppress the effects of electron backscatter. He concludes that the measurements of Proton and Sokol are consistent and therefore, the backscattered electrons did not affect the Proton measurements.

Much of the available data below 1 TeV are also shown in figure 2. As can be seen in this figure, the data between 100 GeV and 1 TeV are sparse. It is also unclear whether there is a spectral feature in the energy range from 100 GeV to 10 TeV as suggested by the Proton satellite spectrum (solid line) or the passive calorimeter data of Zatsepin et al., (1993) which is fit by the dashed curve. If the spectrum does not steepen until 40 TeV as suggested by Asakimori et al. (1993), based on their data, then it appears that there may be a discontinuity in the spectrum in the energy range between 1 and 10 TeV because the flux level in the 100 GeV to 1 TeV energy range appear to be somewhat above the level of the first two data points reported by the JACEE team near 10 TeV.

The cause of the apparent inconsistencies in the data presented in figures 1 and 2 could be: 1) a real spectral feature in the 100 GeV to 10 TeV range; 2) an instrumental effect; or 3) due to the fundamental difference in the nature of the data obtained by thin calorimeters. This third point deserves a careful discussion. It is important to realize that the spectral data points from these devices have a somewhat different meaning than data points from other instruments. Thin calorimeters do not measure the energy of the protons that strike them. In fact, the measurements in these calorimeters give only a poor estimate of the energy of each individual proton. This is because thin calorimeters generally observe only the energy, ΣE_γ, that appears in the form of gamma rays from the first interaction of the incident proton. The fraction of the incident proton's energy that is measured is determined by the partial inelasticity fraction, k_γ, of the proton's first (and usually only) hadronic interaction in the calorimeter. The distribution of k_γ, $f(k_\gamma)$, is shown in figure 4 of Parnell et al. (1989). This distribution extends from 0.0 to more than 0.5, so the conversion factor, X, from ΣE_γ to the proton incident energy, E_p, (i.e. $E_p = X\ \Sigma E_\gamma$) can range from 2.0 to infinity!. While these experiments measure E_p poorly, they measure ΣE_γ to an accuracy of 25% or better. It can be easily shown (Burnett et al, 1986) that in the case where the proton spectrum is a power law in energy and C is energy independent, the proton spectrum plotted versus ΣE_γ will have the same spectral slope as would be the case if Ep had been measured instead. Thin calorimeters, therefore, are suitable for measuring the slope of a power law spectrum. Two difficulties arise however. The first concerns how spectral features in the differential E_p energy spectrum are expressed in the differential ΣE_γ spectrum. The effect of the broad distribution of partial inelasticities, $f(k_\gamma)$, will to broaden and distort the feature. This may influence the interpretation of the spectral features reported by various authors in the proton spectrum. The second difficulty concerns the accuracy of the scale factor $C(k,\gamma)$ for scaling an energy axis expressed in ΣE_γ to one expressed in E_p. This conversion factor is derived taking into consideration the partial inelasticity distribution, the design and composition of the calorimeter, the point of interaction within the calorimeter, and the slope of the cosmic ray spectrum (Burnett et al., 1986). It also rests on some assumptions concerning the gamma ray/charged hadron energy partition. These assumptions result in a systematic uncertainty in $C(k,\gamma)$ of perhaps 20% (Burnett et al, 1986). Such a systematic shift in the location of the thin calorimeter data points on the horizontal axis in figure 2 will have a small effect on the comparison of these data with the data of the other experiments. One must, however, also consider the effect of this systematic error on the location of these data points on the vertical axis. In figure 2, the vertical axis is scaled by $E^{2.7}$. The same 20% systematic error, if it resulted in a systematic overestimate of Ep, would require a correction that would shift the data points from the thin calorimeters down to 0.55 of their plotted values while shifting their energy lower by a factor of 0.8. That shift is nearly enough to bring the passive calorimeter data points into agreement with the spectrum measured by the Proton experiment shown as the solid line in figure 1! There is no way to know if the systematic is this large or if it results in an overestimate of E_p, but the potential impact of this systematic uncertainty must be kept in mind when comparing data from instruments that measure E_p directly with those that measure ΣE_γ.

We contend that the considerations discussed above are sufficient reason for a careful re-examination of the energy range from 100 GeV to 10 TeV and an investigation of the systematics in thin calorimeter measurements. In the next sections we describe our proposed investigations.

1.4 The Total Ionization Calorimeter (TIC)

Our proposed approach to examining the energy range from 100 GeV to 10 TeV for a departure from the power law spectral form is a simple one. We propose to measure of the cosmic ray all particle spectrum in this energy range. The strategy is to make a high statistics measurement with a simple instrument that is not subject to the effects of electron backscatter. We will rely on the fact that in this energy range, the protons comprise about 40% of the all particle flux (Ivanenko, 1993) and that the spectra of the other other elements are much better known than the proton spectrum (Buckley, 1994). As present measurements have already shown, the spectra of all the elements except hydrogen do not steepen in this energy range (Swordy, 1993). If the proton spectrum follows a power law form in this energy range, we would expect the all particle spectrum to also follow a power law or perhaps flatten due to the flattening of some of the other elemental spectra.

Figure 3 (taken from Grigorov, 1990) shows the Proton measurements of the all-particle spectrum in this energy range together with the sum of the elemental spectra measured in the Sokol experiment in his version. The data show a strong indication of a steepening of the all particle spectrum near 1 TeV followed by a flattening near 10 TeV. If this result is correct, it indicates the presence of a spectral feature in this energy range in one or more of the constituent elemental spectra, presumably in the proton spectrum. The spectrum measurements in figure 3 are, however, not in agreement with other measurements (e.g. Ivanenko et al, 1990 and Linsley, 1983).

The all-particle spectrum shown in figure 3 was measured using the the main calorimeter block of the SEZ-14 instrument flown on the Proton Satellites (shown in figure 4) operating as an independent self-triggering calorimeter. This simple instrument has a large geometry factor. Also, because it uses none of the detector elements external to the calorimeter, the backstattered electrons that may plague the other modes of this instrument cannot affect these measurments. The result is a high statistics measurement of the all-particle energy deposition spectrum.

We have modeled the TIC instrument (shown in figure 5) on this portion of the SEZ-14 instrument. Any cosmic ray passing through the TIC calorimeter in any direction will be recorded if it deposits enough energy in the calorimeter. The mean pathlength of a cosmic ray in the TIC calorimeter is:

$$l = (\rho/\lambda)\int_0^\infty s\ p(s)\ ds = 1.17$$

in proton interaction mean free paths, where ρ is the density of the calorimeter and λ is the proton interaction mean free path. The functon p(s) is the probability density that the cosmic ray will traverse the calorimeter along a path of length s (Pickel and Blanford, 1980). In the same way, we find that the mean thickess of TIC is 11 radiation lengths.

It is important to note that TIC does not measure the all-particle energy spectrum, but the all particle energy deposition spectrum instead. Burnett et al. (1986) have shown that if the cosmic ray differential energy spectrum is given by a simple power law relation, then the cosmic ray differential ΣE_γ spectrum is also given by a power law with the same spectral index. The same argument applies to the relationship between the cosmic ray differential energy spectrum and the cosmic ray differential energy deposition spectrum. as Burnett et al. show, these two spectra are related by a normalization factor

$$F(\gamma) = \int_0^1 k^\gamma f(k)dk$$

where k is the fractional energy deposition of a cosmic ray and f(k) is the distribution of energy depositions. It is important to point out that in order to find the spectral index of the power law that best fits the all particle spectrum we need not know $F(\gamma)$, since this spectral index can be found by fitting the energy deposition spectrum.

Our aim in this work is, however, to look for evidence of deviations from the power law form. The approach we have chosen biases us toward measuring a spectrum that can be fit by a power law because the width of the f(k) distribution tends to smooth out deviations from this spectral form. The effect is to make any statistically significant deviations which indicate deviation from a power law more compelling. The scale factor which converts an energy deposition spectrum to a energy spectrum (following the notation of Burnett et al. (1986)) is

$$C(k,\gamma) = \left[\int_0^1 k^\gamma f(k)dk\right]^{-1/\gamma}$$

f(k), in our case is a convolution of the partial inelasticity distribution (since TIC is a thin calorimeter with mean thickness of 1.17 proton interaction mean free paths and 11 radiation lengths) and the pathlength distribution of cosmic ray trajectories through TIC. We propose to determine f(k) using the GEANT code (Brun et al., 1987) which was developed at CERN to model the energy depositions of protons in particle physics experiments including calorimeters. GEANT will allow us to extimate $C(k,\gamma)$. In order to really understand the response of the TIC instrument to deviations in the cosmic ray spectrum, we will use GEANT to investigate the response of TIC to various deviations from a power law. We will also use it to account for the effects of cosmic rays that interact in the calorimeter, the surrounding parts of the experimental apparatus, and the atmosphere.

The TIC detector which will be used for this measurement is shown in figure 5 and figure 6. It consists of five steel plates that are 30 cm square and 7 cm thick. Each plate is followed by a 1 cm thick scintillator. The entire detector is 40 cm high and 30 cm on each side. It is viewed by two 15 cm diameter PMTs. The PMT signals are feed to summing amplifiers and simultaneously routed to discriminators followed by a coincidence unit. When there are coincident signals from the PMTs, the outputs of the four pulse amplifiers are each gated into a 256-bit ADC. The outputs of these ADCs are routed to the external telemetry interface and to internal storage. The data routed to internal storage are mapped into a 28 channel logarithmic spectrum and accumulated in a spectrum memory. Periodically the accumulated spectrum is dumped to onboard recording devices and the spectrum memory is erased. The data routed to the external telemetry interface is also mapped into a logarithmic spectrum and staged to balloon telemetry system for transmission to the ground.

TIC is calibrated using cosmic ray muons at sea level. This is done by placing the calorimeter in a charged particle telescope that defines the muon trajectories and insures that the exiting muon is not accompanied by any secondaries that would have resulted from an interaction in the calorimeter. In this way, we detemine the response of the photomultipliers to the signal of a single relativistic singly ionized particle. The signal from the cosmic ray shower in the calorimeter is just made up of multiple signals from relativistic singly ionized particles, Since the tracks of these particles are physically well separated on an atomic scale as they pass through the scintillators, their signals combine additively. In addition to the muon calibration, the electronic system is checked for linearity over the required dynamic range and for adequate temperature compensation.

The TIC experiment has been flown twice on test flights of the Long Duration Balloon (LDB) system which is under development by NASA for flights around the north pole. In both flights, the data were only recorded internally and examined after recovery of the payload. In the first flight, the balloon burst before reaching float, so only a few hours data were acquired. These data showed that the TIC instrument was performing correctly and prompted us to make some adjustments in the detector threshold and the frequency of internal storage dumps.

The second test flight with the LDB System was been completed on 20 August. We obtained 74 hours of data at float altitude. As of this writing, the payload recovery operations are still in progress and the data from this flight have not yet been examined. We plan to analyze the data from this flight and make any further adjustments in the instrument that may be needed before the 1995 flight. In preparation for the 1995 flight, we will install a inteface between TIC and the balloon control system to telemeter the data to the ground. We are also proposing to calibrate TIC at Fermilab using an external proton beam near 1 TeV. Such a calibration would give us an end-to-end test of our previous calibrations and computer modeling. We hope to do this calibration before the 1995 flight.

In the summer of 1995, NASA plans to attempt the first circumpolar balloon flight in the northern hemisphere. We propose to fly the TIC instrument on this flight. The duration of the flight is difficult to estimate, but it is expected to be in excess of 10 days. Based on the geometry factor of TIC (which is 1 m^2 ster), the probabilities that a cosmic ray will survive passage through the atmosphere and interact in TIC, a 10 day flight and the present measurements of the all-particle spectrum (Grigorov, 1990), we anticipate 4.6×10^6 events above 100 GeV, decreasing with energy approximately as $E^{-1.6}$.

1.5 The Roentgen Emulsion Chamber (REC)

As was discussed in section 1.3, there exists a statistically significant systematic difference in the results from the two research groups using thin passive calorimeters. The objective of this part of the investigation is to investigate if the different designs of the JACEE and MUBEE (Russian) emulsion chambers can lead to this difference. In the course of this investigation we hope to gain a better understanding of the instrumental effects and systematics in thin calorimeters.

The JACEE chambers are described in Burnett et al. (1986) and Parnell et al. (1989) The chambers are designed to have the first interaction occur in a target chamber which consists of acrylic sheets. This target is designed to allow the secondary photons from π^0 decay to reach the calorimeter below without beginning the electromagnetic cascade. In this way, it is expected that the transverse momentum of the π^0's from the interaction of the cosmic ray proton will spread the π^0-decay photons enough to produce separated showers in the lead calorimeter below. When an event behaves in this way, it is possible to measure the cascade energy, ΣE_γ, accurately because the distribution of energy in the cascade of each individual photon can be better simulated and the measurements of the cascade can be better matched to the simulated profile of the shower. There are, however some disadvantages to this approach. The first is that it generally leads to a higher detection threshold for showers, since the shower energy is divided into several separate cascades. Second, not all events behave in this way. Sometimes the gamma rays do not produce well resolved showers; there are showers that begin in the target chamber; secondary interactions of the hadronic core that contribute; and, of course, there are the protons that don't interact until they reach the Pb calorimeter.

In contrast, the MUBEE chambers do not employ a separate target chamber. They consist of only of Pb sheets and the various detectors (emulsions, x-ray films, etc.). In these chambers, the showers due to the individual gamma rays are never resolved. All the shower energy is deposited in a single undifferentiated shower. This has the advantage of a lower detection threshold, but probably suffers from a lack of knowledge of how much energy is hidden in the saturated core of a shower.

In order to address the detector uncertainties, REC will be comprised of both types of emulsion chambers. The tracks recorded in each kind of chamber will be subjected to the same measurement methods and both will be modeled with the same Monte Carlo simulation codes. The aim will be to discover if the disagreement between results obtained in these two kinds of chambers are due to systematic effects that have not been understoood.

The REC design will consist of four of chambers. An example of the design of one of these chambers is shown in figure 7. Each will have a target block (M-block) and lead calorimeter block (G-block). Thin (50 μm) layers of nuclear emulsion of R-2T-50 type and X-ray films of RT-6-1 type are used as the radiation detectors. The chambers will be of two types. The M-block of the first type chamber (carbon-chamber) is composed of ~50 plexiglass plates of 2 mm thickness interleaved with nuclear emulsions. It should be noted that low Z material, such as plexiglass, allows one to have a high probability of nuclear interaction with a low probably of pair production by high energy gammas from π^0 decay. With this type of chamber, the individual interactions of primary cosmic ray particles with the carbon nuclei can be examined in more detail. M-blocks of this design will have about 0.2 of an interaction mean free path for protons and they will present about 0.3 radiation lengths to the secondary gamma rays. In addition to the nuclear emulsions in these M-blocks, we will insert CR-39 track detectors so that the tracks of Z>9 primary particles or fragments can be detected, and their charges can be measured. G-blocks are 7 radiation lengths thick. They consist of ten lead plates of 1 mm and five plates of 5 mm thickness. The Pb plates alternate with nuclear emulsion and X-ray films in these blocks.

For the second type chamber, lead plates are used in the M-blocks as target layers in which the interaction of primary cosmic particles take place. The entire chamber consists of 20 thin lead layers of 1mm thickness and 9 thick lead plates of 5mm thickness. If 7 lower plates of this chamber are considered as being the G-block, the total thickness of M-block will be about 0.2 of a proton interaction length. A rapid cascade evolution in lead makes the examination of individual interactions in such a chamber difficult.

The procedure used for following and measuring events is described next. The primary cosmic rays striking a REC chamber may interact with nuclei in the M-block target sheets. The secondary charged particles from the interaction are registered in lower nuclear emulsions as narrow bundle of tracks. The high energy gamma rays from the π^0-decay will start electromagnetic cascades in lead plates of G-block. The cascades are observed in the x-ray films of the G-block as dark spots and are easily detected by naked eye. The identification and selection of the events is performed by finding the total energy all the gamma rays from the π^0-decays, ΣE_γ. ΣE_γ must exceed a threshold energy for the event to be accepted. By tracing each cascade through successive nuclear emulsion films up to vertex of the primary cosmic ray interaction, we find the primary particle and identify its charge. The procedure of tracing demands exact film registration in the chamber. The initial registration accuracy is about 0.5 mm. A microscope-video-camera-computer system at the Lebedev Institute in Moscow will be used by us to improve the registration to an accuracy of 50-60 μm. With this accuracy we expect to be able to find the primary particle track in all the upper nuclear emulsion films.

Measurement of the primary cosmic rays' charge are performed in the nuclear emulsion by several methods depending on charge and the angle of incidence. We will use one or more of the following methods:

-grain (or blob) counting,
-gap (lacunarity) measurements,

-delta ray counting,
-scanning photomicrodensitometry of the emulsion track

In addition, for nuclei with Z>9 and angles near vertical incidence, the CR-39 etch-pit measurements will be used. The cascade energy determination is made by measuring an optical density of dark spots produced by a cascade in the X-ray films. These measurements are compared with the calculations performed using cascade theory. The energy spectra of the primaries are obtained from by scaling the cascade spectra with a factor obtained from the partial inelasticity of the primaries' interactions. At the lower energy the determination of cascade energy is carried out by track counting method in nuclear emulsion. This method is time-consuming but guarantees a better accuracy in energy measurements when optical photodensitometry does not provide sufficient accuracy in the lower energy region, i.e. when the optical density of dark spots approach the x-ray film background fluctuations.

Using the carbon-chamber modules, we plan also to measure the following characteristics of nucleus-nucleus interactions:

-the charge of primary particle;
-the number of secondary charged particles and gamma-quanta, emitted to forward cone;
-emission angles of secondary charge particles and gamma rays;
-energies and transverse momenta of secondary gamma rays;
-energy sum of secondary charge particles and gamma rays.

The analysis of nucleus-nucleus interactions can provide information about new phenomena that are not expected in proton-nucleus interactions such as: superposition and collective interactions; quark-gluon plasma formation; special types of events which generate high transverse momentum particles (e.g. Apanasenko et al., 1990).

On the planned 1995 flight around the north pole, we propose to fly four emulsion chambers at an altitude of > 30 km for ≥200 hours. The total area of the four chambers is 1 m^2 and the total weight is 700 kg. We suppose that the accumulated factor of the exposure for proton and helium will be:

primary particle	$A\Omega\eta wt$ in m^2 hour ster
p	75
He	99

where η denotes the fraction of the cosmic ray flux that interacts the residual atmosphere and "w" denotes the probability of an interaction in the emulsion chamber.

Two REC modules, one of each type described above, were flown on the LDB test flight that was just completed. These modules were exposed for 74 hours at > 30 km. The data from these modules will be examined before preparing the modules for the 1995 flight and adjustments, if needed, will be made in the preparations for the 1995 flight. We will also procure, test and calibrate the detectors that are to be used in the 1995 flight.

1.6 The Balloon Flight

We anticipate having NRL, MSU and RAS personnel on site in Inuvik for launch preparations which will include integration of the passive detectors into the REC modules. One NRL representative will remain on site in Inuvik until after the launch while another NRL representative will be on site at the Remote Operations Center (ROC) in Palestine. After the launch, NRL will maintain a presence at the ROC to monitor the instrument performance and analyze data from TIC. TIC data will also be forwarded to MSU by electronic mail for analysis.

MSU and RAS will have personnel on site in Sandrestromfjord, Greenland to participate in recovery and disassembly of the REC and TIC instruments after the flight.

Following the flight, the data from TIC will be analyzed jointly by NRL and MSU. The a CR-39 detectors will be processed and measured at NRL. The emulsions and x-ray films from REC will be processed, scanned and measured at RAS. The locations of heavy ions will be sent to NRL for charge analysis in the CR-39 detectors.

2.0 REFERENCES

Akimov et al., 1969, 11th ICRC (Budapest), OG-99.
Apanasenko, A.V. et al., 1991, Proc. 21st ICRC (Adelaide), **8**, 112.
Asakimori, K. et al., 1991, 22nd ICRC, **2**, 97.
Asakimori, K. et al., 1993, 23nd ICRC, **2**, 21.
Buckley, J., Dwyer, J., Muller, D., Swordy, S., and Tang, K.K., 1994, Ap.J., **429**, 736.
Burnett, T.H. et al., 1986, NIM, **A251**, 583.
Burnett, T.H. et al., 1990, ApJ., **349**, L25.
Brun, R. et al., 1987, "GEANT3 User's Guide", CERN Data Handling Division, DD/EE/84-1.
Drury, L.O'C, Volk, H.J., and Mariewicz, W.J., 1989, Astron. and Astrop., 225, 179.
Ellsworth, R.W. et al., 1977, Astrophy.Sp.Sci., **52**, 415.
Gaisser, T.K. et al., 1990, "Cosmic Rays and Particle Physics", Cambridge Univ. Press.
Grigorov, N.L., 1990, Sov. J. Phys., **51**, 99.
Grigorov, N.L. et al., 1989, Moscow State Uni.USSR, Inst.Nuc.Phys., **preprint 89-58/135**.
Grigorov, N.L. et al., 1989, Cosmic Rays Research, 305-310.
Grigorov, N.L. 1989, Cosmic Rays Research, 484-488.
Grigorov, N.L. et al., 1989, JETP Lett., **49**, 278.
Grigorov, N.L. et al., 1989, JETP Lett., **49**, 83.
Grigorov, N.L. et al., 1972 "Space Research", (Berlin), Akademik-Verlag, **XII**, 1617.
Grigorov N.L. et al, 1970, Yadernaya Fizika, **11**, 1058.
Grigorov, N.L. et al., 1967, Aca.Sci. USSR, Lomonosov State Uni. Moscow.
Gupta, M., and Webber, W.R., 1989, Ap.J., **340**, 1124.
Ichimura, M., et al., 1993, Proc. 23rd ICRC (Calgary), **2**, 9.
Ivanenko et al., 1993, Proc. 23rd ICRC (Calgary), **2**, 17.
Ivanenko et al., 1990, Proc. 21st ICRC (Adelaide), **3**, 77.
Jokipii, J.R., 1987, Proc. 6th Solar Wind Conf., NCAR TN-306, **2**, 481.
Jones, W.V., 1969, Phys.Rev., **187**, 1868.
Jones, W.V., 1970, Acta Phys.Aca.Sci.Hungaricae 29,Suppl.4, 513.
Jones, W.V., 1970, Acta Phys.Aca.Sci.Hungaricae 29,Suppl.4, 505.
Juliusson, E., Meyer, P. and Muller, D., 1972, Phy.Rev.Lett., **29**, 445.
Linsley, J., 1983, Proc. 18th ICRC (Bangalore), **12**, 135.
L'Heureux, J. et al., 1990, Nuc.Ins.Metho.Phys.Res., **A295**, 246.
Muller et al., 1991, Ap.J., **374**, 356.
Parnell, T.A. et al., 1989, Adv.Space.Res., **9**, 45.
Pickel, J.C., and Blanford, J.T., 1980, IEEE Trans. on Nucl. Sci., **NS-27**, 1006.
Review of Particle Properties, 1990, Phys.Lett.B., **239**.
Ryan, M., Ormes, J.F., and Balasubrahmanyan, V.K., 1972, Phys. Rev. Letters, **28**, 15.
Swordy, S.P., 1993 in "Invited, Rapporteur & Hightlight Papers", Proc. 23rd ICRC (Calgary), 243.
Swordy, S.P. et al., 1990, Ap.J., **349**, 625.
Swordy, S.P. et al., 1993, ApJ., **403**, 658.
Vernov, S.N. et al., 1983, Aca.Sci.USSR, Lebedev Phys.Inst., **preprint N230**.
Wiebel, B., 1994, thesis.
Zatsepin, V.I., 1993 in "Invited, Rapporteur & Hightlight Papers", Proc. 23rd ICRC (Calgary), 249.
Zatsepin, V.I., et al., Proc. 23rd ICRC (Calgary), **2**, 13.

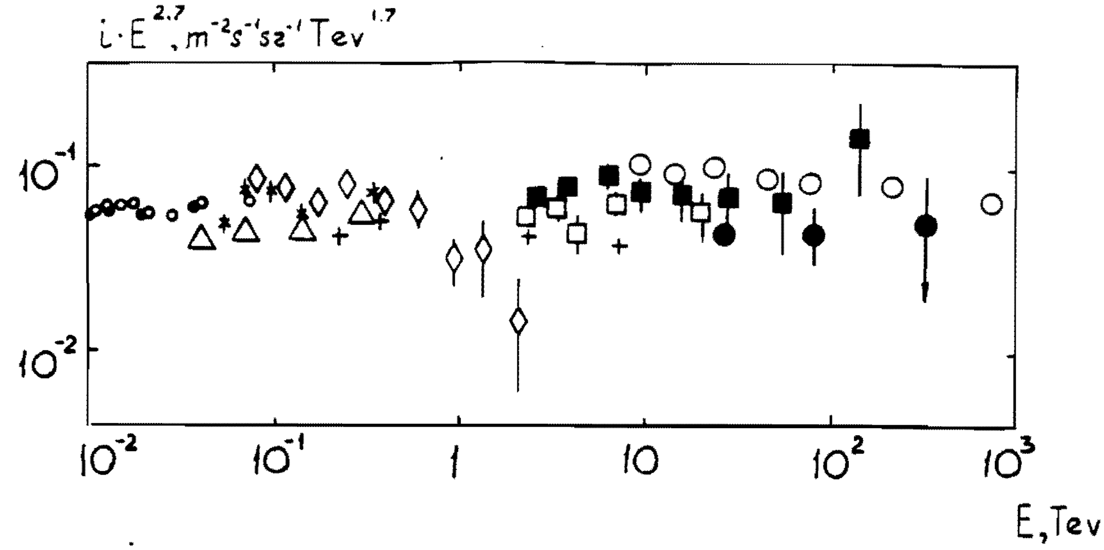

Fig.2. Helium nucleus spectrum.
○ ● - 3, △ - 4, ◇ - 5, × - 10, + - 2,
□ - 6, ■ - 7, ○ - 8, ● - 1.
E is the energy per nucleus.

Figure 1: The Differential Cosmic Ray Helium Spectrum in Energy per Nucleus (taken from Zatsepin, 1993). The data points come from: ([1]) Zatsepin et al. (1993); ([2]) Grigorov et al. (1970); ([3]) Webber, Golden and Stephens (1987); ([4]) Seo, Ormes and Streitmatter (1991); ([5]) Ryan et al. (1972); ([6]) Grigorov (1990); ([7]) Ivanenko et al. (1990); and ([8]) Asakimori et al. (1991).

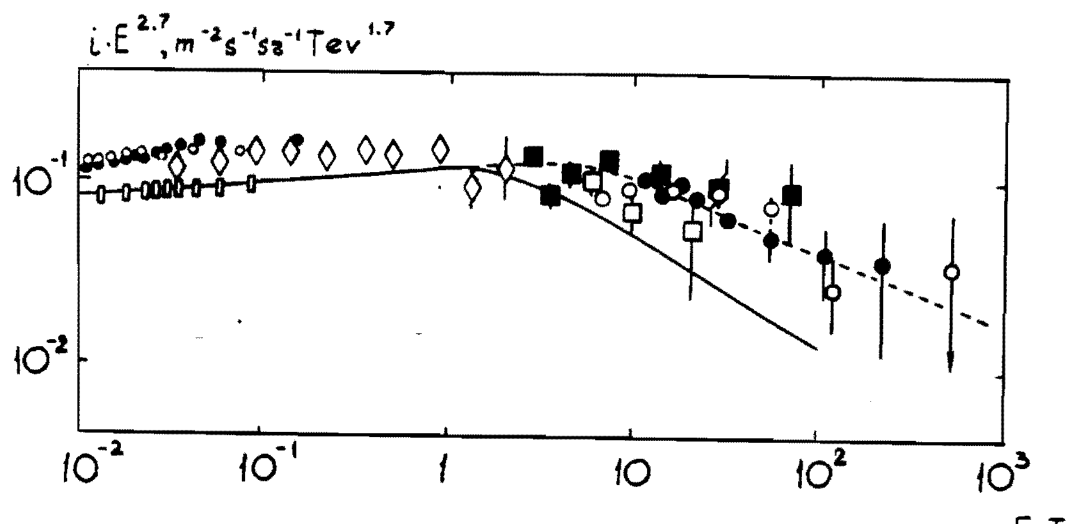

Fig.1. Differential energy spectrum of protons.
○ ● - 3, ▯ - 4, ◇ - 5, □ - 6,
■ - 7, ○ - 8, ● - 1.

Figure 2: Cosmic Ray Proton Differential Energy Spectrum (taken from Zatsepin, 1993). The data points are taken from: ([1]) Zatsepin et al. (1993); ([3]) Webber, Golden and Stephens (1987); ([4]) Seo, Ormes and Streitmatter (1991); ([5]) Ryan et al. (1972); ([6]) Grigorov (1990); ([7]) Ivanenko et al. (1990); and ([8]) Asakimori et al. (1991). The solid curve is a fit to the Proton Satellite measurements of Grigorov et al. (1970) and the dashed curve is a fit to the measurements of Zatsepin et al. (1993).

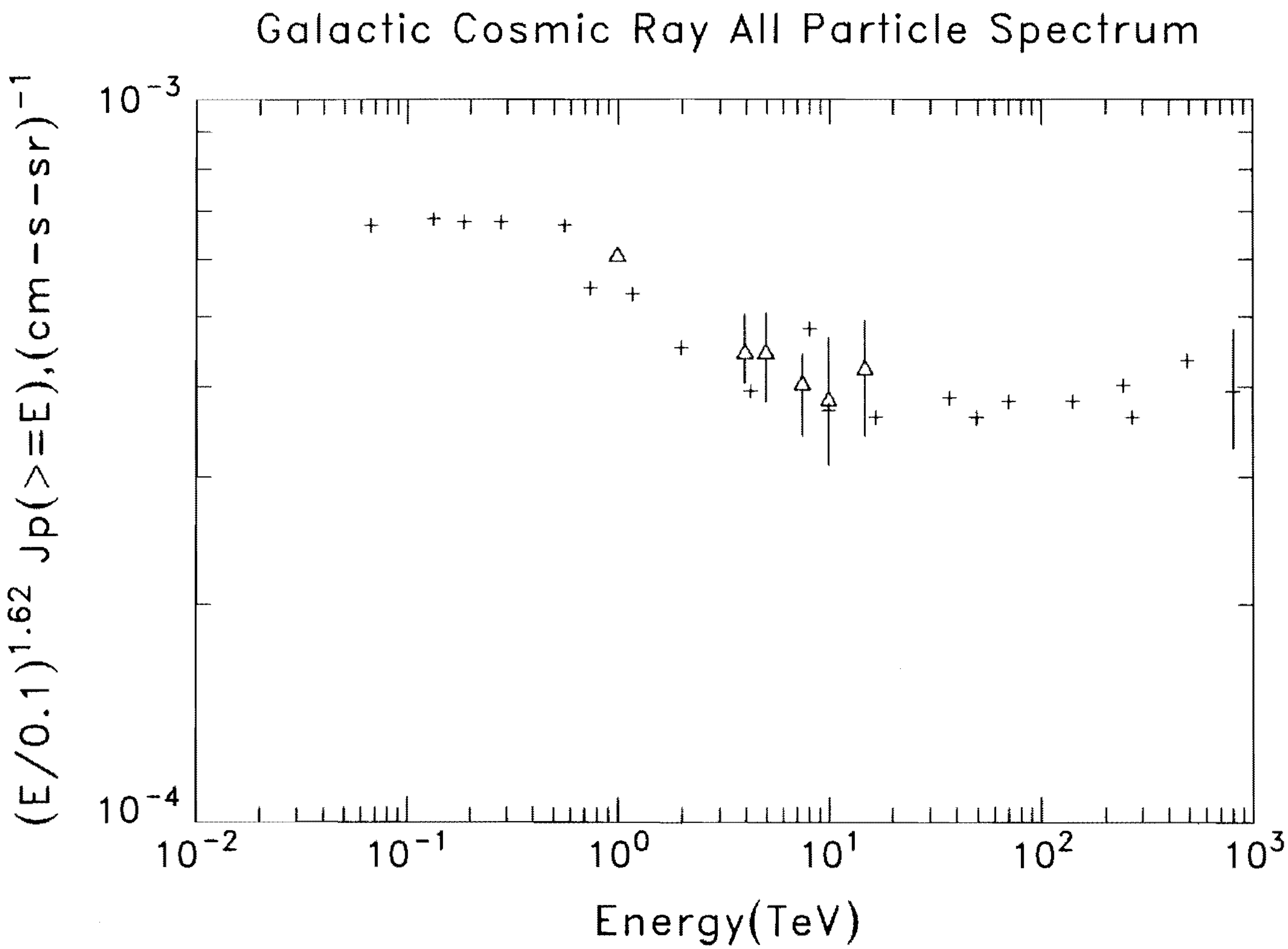

Figure 3: This figure is taken from Grigorov (1990). It shows measurements of the galactic cosmic ray all particle spectrum from the Proton Satellites (+'s) and from the sum of the elemental spectra measured in the Sokol experiment (triangles).

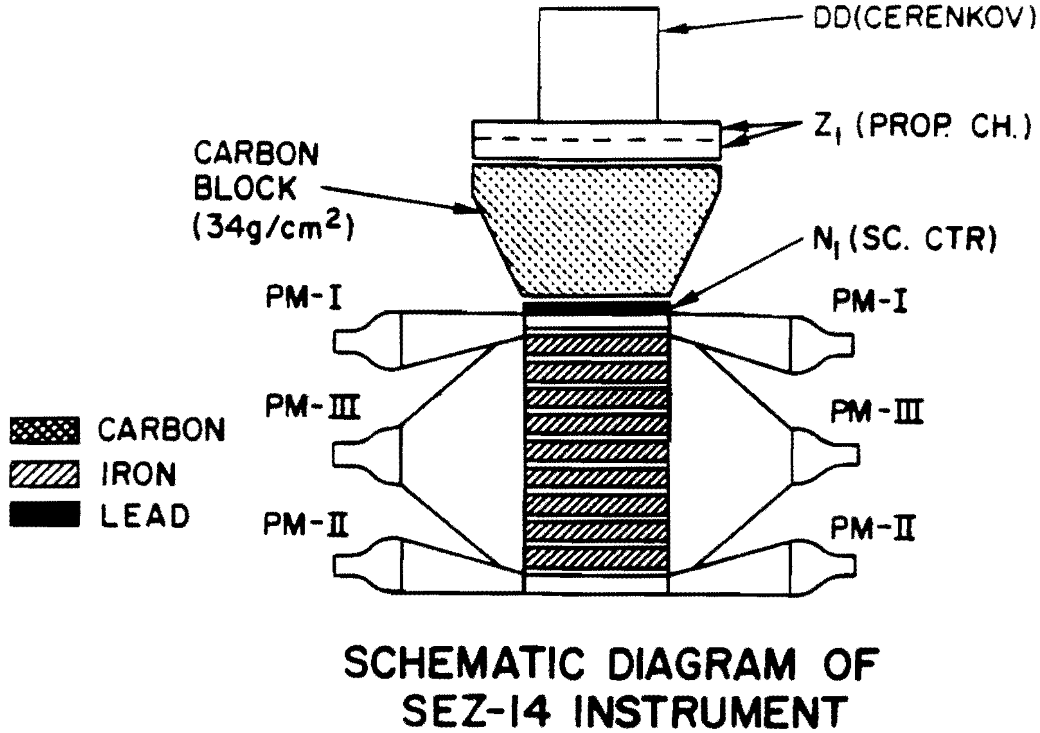

Figure 4 : This figure shows the SEZ-14 cosmic ray calorimeter flown on the Proton Satellites. The all-particle spectrum measurements were made with the central iron calorimeter that is viewed by the two photomultiplier tubes labeled PM-III in the figure.

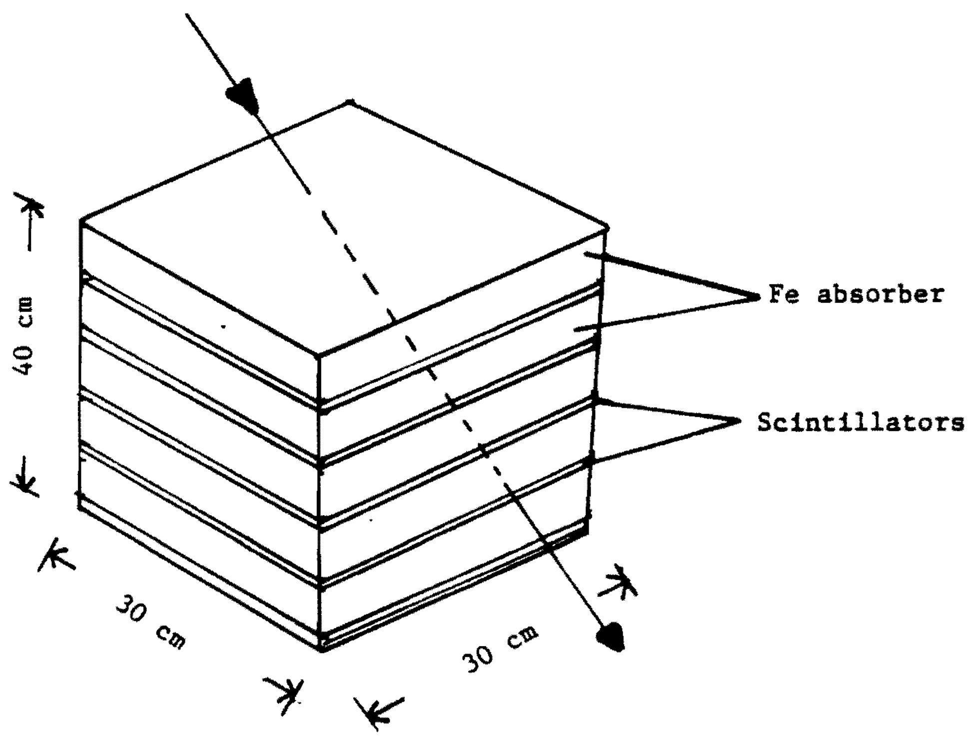

Figure 5: The calorimeter of the TIC instrument. This calorimeter consists of five iron plates, each 7 cm thick and each followed by a 1 cm thick scintillator.

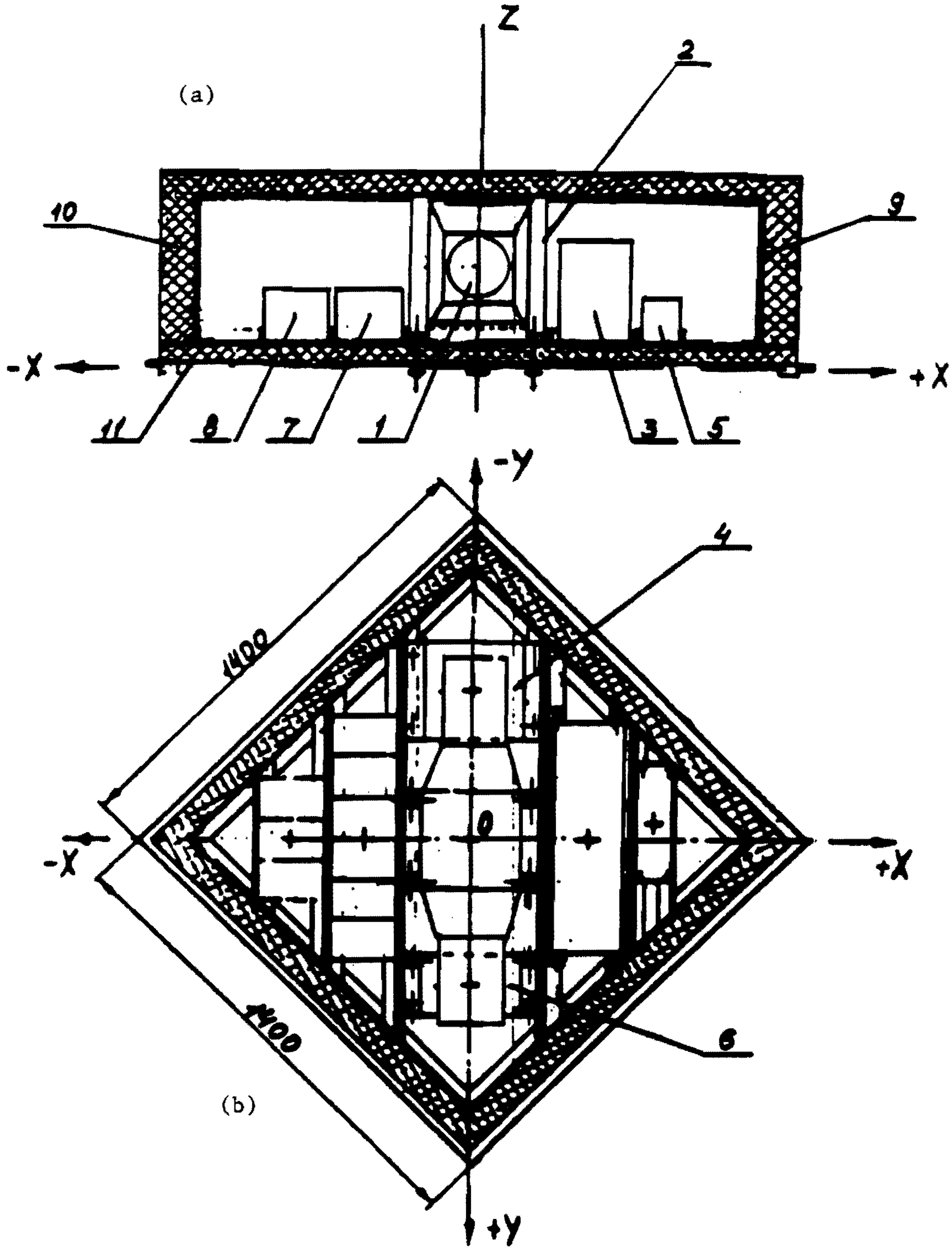

Figure 6: The TIC instrument shown in a side view (a) and a top view (b). The dimensions are in millimeters. The components of the instrument are: 1) a phototube; 2) the calorimeter; 3) the onboard data recording system; 4) and 6) the two phototubes; 5) The central electronics and SIP interface; 7) and 8) batteries; 9) copper EMI shield enclosure; 10) foam insulation; and 11) wooden pallet base.

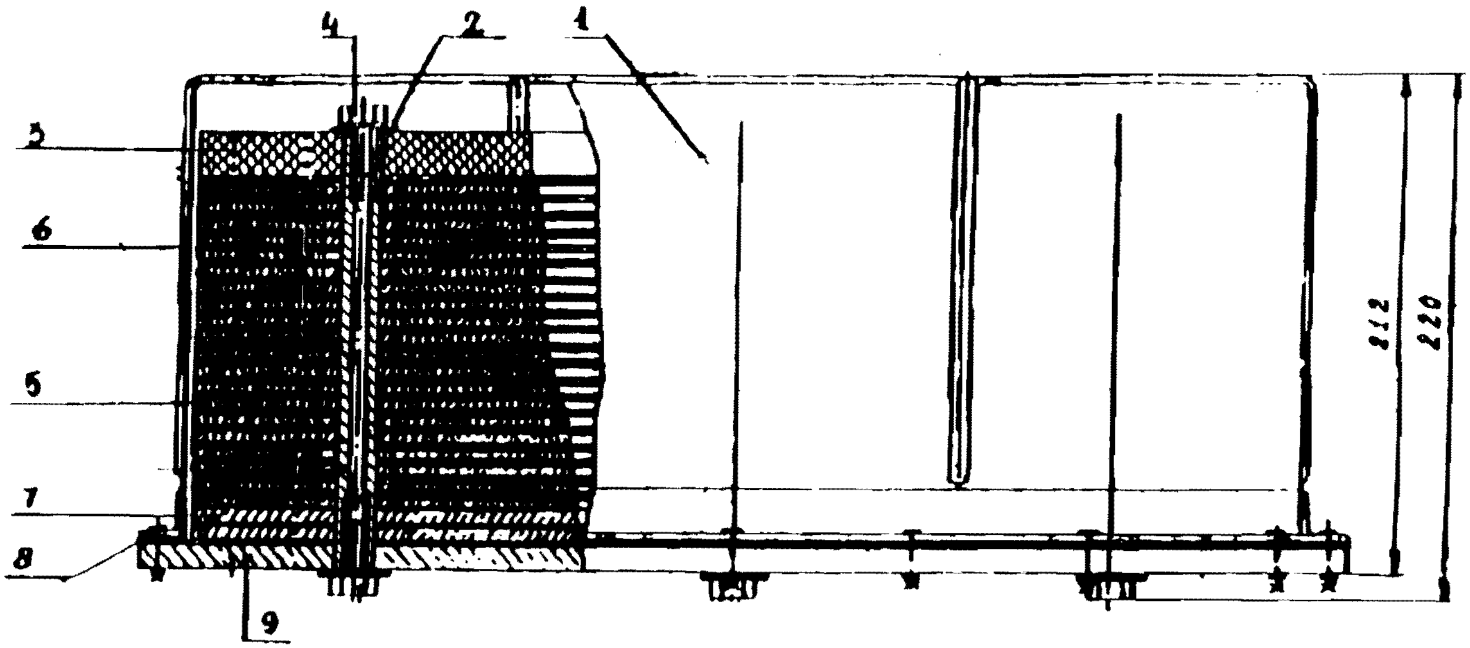

Figure 7: Roentgen Emulsion Chamber. The Chamber consists of 1) air tight cover; 2) Washer; 3) clamp plate; 4) dowel; 5) G-block; 6) M-block; 7) thick Pb sheets of the M-block; 8) gasket; and 9) base plate.